Proceedings of IMECE '03:
2003 ASME International Mechanical Engineering Congress and Exposition
Washington, D.C. -- November 16-21, 2003

IMECE2003-42178

CORRELATIONS BETWEEN SPRAY PROPERTIES AND HEAT TRANSFER DYNAMICS DURING CRYOGEN SPRAY COOLING

Odette Ma[1], G. Aguilar[1,2,Ψ] and J. S. Nelson[1]

[1]Beckman Laser Institute
University of California, Irvine, CA 92612

[2]Department of Mechanical Engineering
University of California, Riverside, CA 92521

G.-X. Wang

Department of Mechanical Engineering
The University of Akron
Akron, Ohio 44325-3903, USA

ABSTRACT

Cryogen spray cooling (CSC) has been used along with pulsed lasers for nearly a decade to irreversibly photocoagulate a variety of vascular lesions. However, the fundamental mechanisms that take place at the skin surface are still incompletely understood. In this work, we built a fast-response temperature sensor with the objective to determine the time in which liquid cryogen remains on the skin surface during and after a short spurt of cryogen—the residence time (t_r). Measurements are conducted systematically at various distances from the nozzle (z) and various spurt durations (Δt) for two nozzles that produce completely different spray characteristics. It was found that for each nozzle, there is a critical spray distance (z_c) where an abrupt increase in t_r occurs and another critical distance (z_{max}) that can be related to maximal cryogen deposition. Furthermore, using experimentally measured average droplet diameter (d) and velocity (v) for sprays produced by each nozzle, we defined a spray characteristic time $\tau(z)$ as the ratio of d to v. This parameter allows us to represent our experimental data on a single curve for each nozzle, by plotting the dimensionless residence time (t_r/τ) as a function of the product of dimensionless spurt duration ($\Delta t/\tau$) and a dimensionless factor (m/m_{max}). The factor m/m_{max} is envisioned as an effective mass deposition which, due to the evaporation of cryogen droplets in-flight and the spray-surface interactions, is a strong function of z. These results represent a step towards a more complete understanding and quantification of the physics involved in CSC.

Keywords: spray cooling, laser photocoagulation, nozzle characterization.

INTRODUCTION

Laser surgery is effectively used to irreversibly photocoagulate port wine stain (PWS)[1,2] birthmarks and other vascular lesions such as telangiectasias, hemangiomas[3], and rhytides. However, epidermal melanin acts as a non-specific target, absorbing a significant portion of laser light and thus, limiting the dose that can be safely delivered to the underlying targets. Moreover, if laser light absorption within the epidermis is excessive, it can lead to permanent damage such as scarring and dyspigmentation. To avoid this, cryogen spray cooling (CSC) was introduced as a mean to cool the skin prior to laser irradiation [1, 2].

On a different realm, there have been a significant amount of studies on water sprays, from which empirical correlations have been developed to predict various spray characteristics. For instance, Elkobt [4] amongst many others, proposed correlations to estimate the Sauter mean diameter (SMD) of droplets produced by plain orifice atomizers (similar to those used on the cryogenic sprays produced by commercial devices). Unfortunately, none of these correlations accounted for liquid evaporation, which is likely significant during cryogenic sprays. Studies of evaporating liquids, such as fuels have also been carried out [5][6], but almost none of them dealing with the interaction with solid surfaces. Finally, only a few studies on cryogenic sprays have been reported, In particular, Ingebo [7][8][9] worked with two-fluid type nozzles, where a high velocity gas flow was used to atomize the liquid cryogen. He studied the effect of the gas temperature, gas properties, and vaporization on the average spray droplet diameter. However, the nozzles he used were different kinds of atomization devices than those used for PWS treatment.

[Ψ] Corresponding author: gaguilar@engr.ucr.edu

The success of CSC over other cooling methods used for laser therapy of superficial targets is due, in part, to the accurate control of the spray application time (~10 - 100 ms) and the high heat flux (q) induced by the cryogen that evaporates on the skin surface [10]. To this date, there are many studies which report the performance of CSC nozzles, either through the measurement of q and/or heat transfer coefficients (h), using various skin models such as epoxy blocks [11, 12] and metal rods or disks [13, 14] under a variety of spray conditions[11, 13-16] . Unfortunately, the response time of some of these devices is too slow to depict the dynamic variation of the surface temperature during CSC [17].

Fewer studies have dealt with cryogen spray characterization itself. Aguilar *et al.*[18] investigated how spray characteristics such as average droplet diameter (d), velocity (v), and temperature (T) are affected by nozzle geometry, and developed a model to predict evaporation in-flight. Pikkula *et al.*[19] and Karapetian *et al.*[20] correlated some of the spray characteristics, including d and v to q. In the latter study, it was concluded that while d has a small influence on q, v and mass flow rate ($\dot{m}$) are the most influential parameters.

Recently, a fast response sensor was introduced [10, 21] to resolve near "real-time" surface temperature dynamics, including cryogen boiling and evaporation. Furthermore, it was recognized that spurts impacting the surface in a jet-like fashion (nozzle positioned less than 25 mm from the surface) led to different surface temperature dynamics compared with those impacting the surface more gently (nozzle positioned more than 50 mm from the surface).

For this study, we selected two nozzles that produce distinct spray characteristics [17] and deliver short spurts on the fast-response temperature sensor. We conduct systematic measurements of surface temperature at various distances from the nozzle (z) and spurt durations (Δt), with the objective to determine if the surface temperature dynamics, particularly the residence time (t_r) can be uniquely related to distinct spray characteristics produced by the two different nozzles, *e.g.*, d and v.

EXPERIMENTAL SET-UP AND PROCEDURES

Nozzles and cryogen delivery

In this study, we used two stainless steel, straight tube nozzles with 0.7 mm and 1.4 mm inner diameters, both of length 32 mm. These nozzles were chosen based on the different spray characteristics they produce, especially at $z < 30$ mm, as documented in previous work [10, 17]. These nozzles are hereafter referred to as narrow (N) and wide (W) for the smaller and larger diameters, respectively. The nozzles are soldered onto a custom made copper coupling that fits tightly around a fuel injector. The cryogen used was 1,1,1,2 tetrafluroethane, which is otherwise known as R134a and has a boiling temperature ($T_b \sim -26°C$) at atmospheric pressure. The cryogen was kept at 660 kPa (saturation pressure at room temperature) and was delivered to the nozzle setup through a standard high-pressure hose attached to an electronically controlled fuel injector.

Fast response temperature sensor

This sensor consists of a 50 μm diameter bead of type-K thermocouple placed over a poly methylmethacrylate (Plexiglas®) substrate bar and covered with a thin (50 μm) aluminum foil (Figure 1).

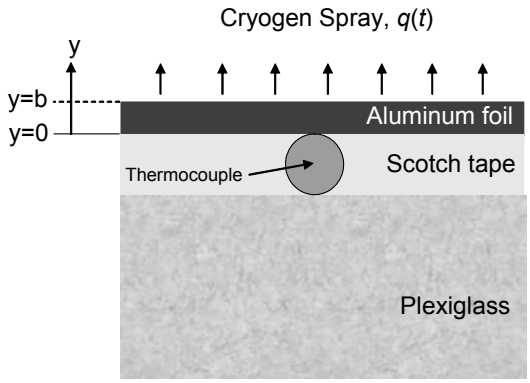

Figure 1. Schematic of the thin Al- foil fast response temperature sensor.

Since the aluminum foil has a very high thermal conductivity and low specific heat compared to Plexiglas®, most of the heat supplied to the cryogen was provided by the Plexiglas® itself, which happens to have skin-like thermal properties, as shown in Table 1.

Table 1: Thermal properties and thicknesses of layers used for the temperature sensor device. Skin properties also provided for reference.

Properties	Al	Scotch Tape®	Plexiglas®	Dermis
Thickness [mm]	0.020	0.050	19	--
K [W/(m K)]	205	0.19-0.25	0.19-0.24	0.54
ρ [kg/m^3]	2,710	1,160	1,150	1,150
c [J/(kg K)]	896	1,400	1,400	3,700
α_{avg} [m^2/s]	844×10^{-7}	1.22×10^{-7}	1.31×10^{-7}	1.26×10^{-7}

Smearing a minute amount of thermal paste on the thermocouple bead ensured good thermal contact between the bead and the aluminum foil. The sensor was exposed to a cryogen spurt at given z and Δt making sure the sprayed area was always smaller than the aluminum foil size, so the measured temperature represents an average of the surface temperature. The sensor's temperature was recorded as a function of time at 4 kHz using an A/D converter board acquisition card and dedicated software (InstruNet™, Omega

Engineering, Stamford, CT). This acquisition rate ensures an appropriate resolution given the thermal response time of the sensor, which considering the size and geometry of the materials used and the average cooling conditions to which it was exposed, we estimated on the order of 5-8 ms. The sensor was allowed to return to ambient temperature before another experiment was performed. In addition, various identical experiments (3-5) were carried out systematically to verify the reproducibility of our results, which was quite remarkable and ruled out the possibility of random errors associated with the sensor's design.

For each spurt duration, the cryogen residence time (t_r) was according to the definition introduced by Aguilar *et al.*[10], where t_r is the time the surface temperature remains below T_b during and after a short cryogen spurt, as illustrated in Figure 2 for the case of a 70 ms spurt at a distance of 20 mm from the surface.

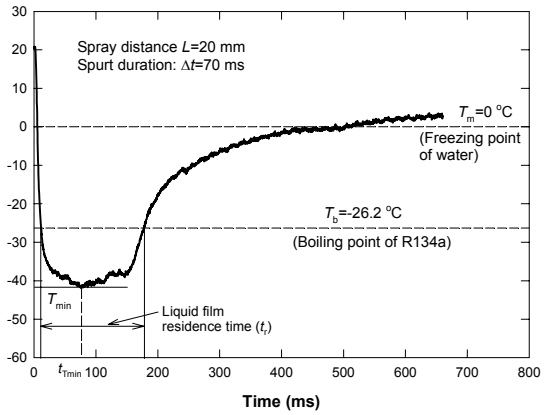

Figure 2. A typical temperature curve as a function of time and definition of residence time, t_r.

Spray Characteristics (diameter and velocity)

A Phase Doppler Particle analyzer (PDPA by TSI Inc., St. Paul, MN) was used to determine the average droplet diameter (d) and velocity (v) at various spray distances (z) from the nozzle tip along the axis of symmetry. This apparatus is based on the principles of light scattering interferometry, and permits simultaneous droplet diameter and velocity measurements over a small (~ 1 mm^3) probe volume formed by the intersection of two off-phase laser beams of the same wavelength [22]. The information provided by this apparatus is fundamental for this work since d and v are the spray properties that may be related to the amount of mass deposited on the sprayed surface and, thus, to the heat transfer dynamics.

We use Sauter mean diameter (SMD or D_{32}) as a meaningful quantity of droplet diameter. SMD represents an average droplet diameter with the same volume to surface area ratio as that of the entire spray. For fuel combustion applications, Lefebvre [23] highly recommends the use of this average diameter, since it is least susceptible to a large spread in the droplet diameter distribution. Since cryogen and fuel sprays are made of droplets evaporating in flight, it seems appropriate to use SMD in the present work.

RESULTS AND DISCUSSION

Temperature Measurements

Figures 3 and 4 show the temperature variations measured for 30 ms spurts produced by the N and W nozzles, respectively, at various z. Two aspects vary noticeably: the minimum temperature (T_{min}) and the resident time (t_r). For both nozzles, T_{min} decreases and t_r increases with larger z, up to some maximum value of z (z_{max}). Beyond z_{max}, T_{min} increases and t_r decreases, suggesting that a good portion of the droplets evaporate completely before reaching the temperature sensor's surface.

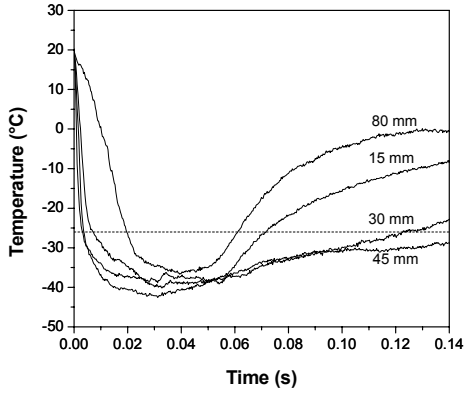

Figure 3. Surface temperature variation with time for N nozzle sprays. Δt = 30 ms.

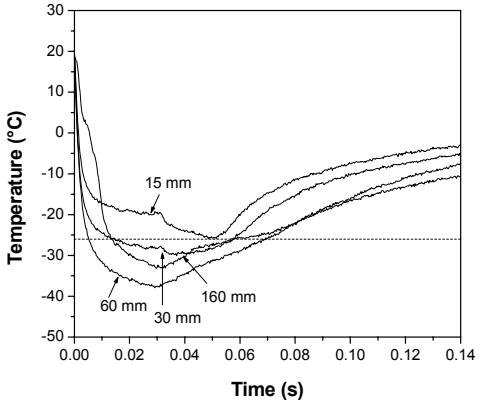

Figure 4. Surface temperature variation with time for W nozzle sprays. Δt = 30 ms.

Critical spray and maximal cryogen deposition distances

Figure 5a shows the variation of t_r as a function of Δt at various z for the N nozzle. The continuous increase in t_r pointed out above is more clearly observed. For z varying

from 15 mm through 35 mm, the increase in t_r seems very gradual. A somewhat larger increase occurs abruptly between z = 35 - 40 mm, suggesting a change in the spray pattern or spray-surface interactions. However, t_r continues to increase up to 45 mm. As z increases beyond 45 mm, t_r decreases, as shown in Figure 5b. This suggests that somewhere around 40 - 45 mm maximal cryogen deposition occurs and therefore, the time it takes for the cryogen to boil and evaporate completely is the longest [10]. Hereafter, we refer to the distance where the abrupt increase is found as the critical distance z_c (35 – 40 mm) and the maximal cryogen deposition distance as z_{max} (40 – 50 mm).

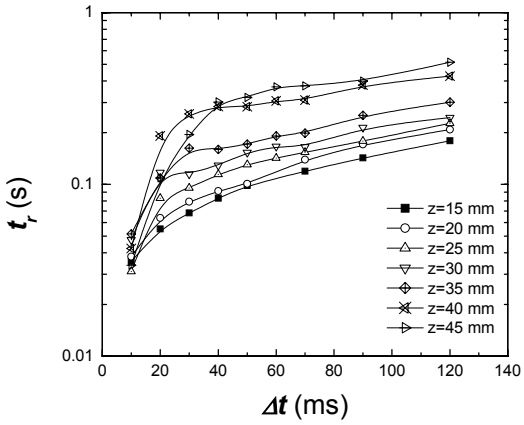

Figure 5a. t_r versus Δt for the N nozzle sprays before z_{max}.

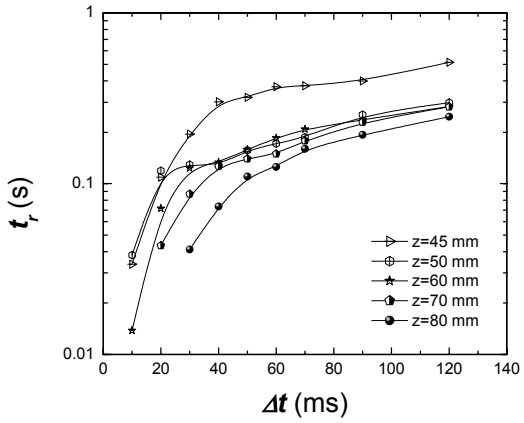

Figure 5b. t_r versus Δt for the N nozzle sprays after z_{max}.

Similar to Figures 5a and 5b, Figures 6a and 6b show the variation of t_r as a function of Δt for various z for the W nozzle. This nozzle produces a very visible jet-like spray with minimal atomization [17], which results in a very forceful impact, significant droplet rebound, and minimal cryogen deposition. Therefore, considerable cryogen spreading and shorter z_c was expected for this nozzle. Similarly, the faster and larger droplets of this nozzle's sprays were expected to reach longer distances and, thus show a larger z_{max}. Indeed, z_c was found to exist between 15 - 20 mm and z_{max} occurred much farther away (~ 160 – 170 mm) compared to the N nozzle sprays.

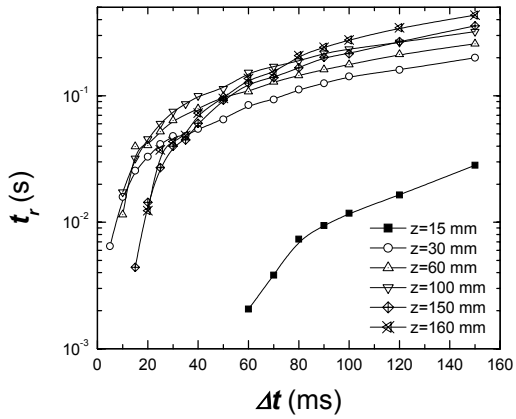

Figure 6a. t_r versus Δt for the W nozzle. Notice that a transition occurs from z=15 mm to 20 mm. t_r reaches a maximal at z_{max} = 160 mm.

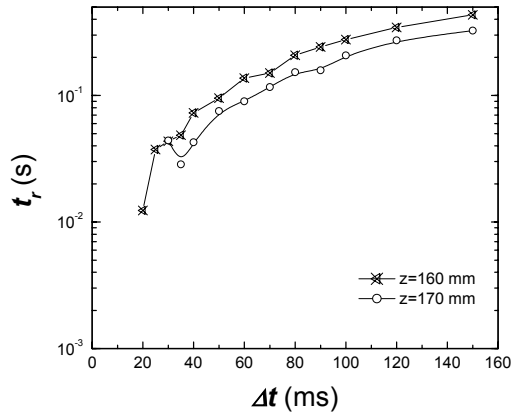

Figure 6b. t_r versus Δt for the W nozzle. Notice that t_r is smaller for z =170 mm than z =160 mm.

Characteristic time (τ) and effective mass deposition (m/m_{max})

It is reasonable to assume that the heat transfer dynamics observed under spurts produced by the N and W nozzles must be ultimately related to the fundamental spray characteristics resulting from each nozzle, such as average droplet diameter (d) and velocity (v). Using the PDPA described above, we measured d and v at various z along the spray cone axis for spurts produced by both nozzles. Using these measurements, we define a spray characteristic time (τ) as the ratio of d and v, $\tau = d / v$. Table 2 summarizes these results and the computed values of $\tau(z)$. The large increase in d seen for z ≥ 85 for the N nozzle is somewhat uncertain. At this distance, most droplets have evaporated and, therefore, the droplet count is too small to provide a good average. Therefore, this data (shaded area) has not been used for the subsequent computations. It is

important to mention, however, that while an increase in d with increasing z may seem counterintuitive, studies of various spray systems have reported that this phenomenon can be attributed to the presence of droplet coalescence [24][25].

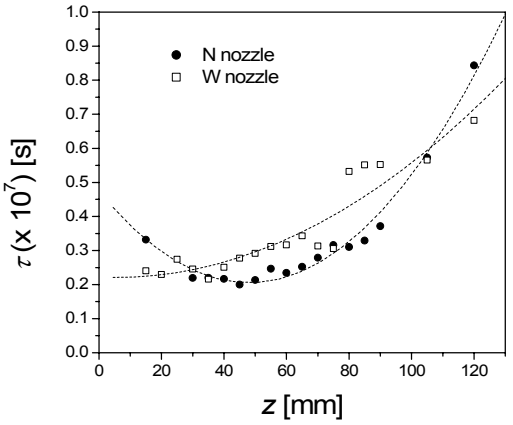

Figure 7. τ *vs.* z for the N (solid) and W (hollow) nozzles, respectively.

Figure 7 shows τ as a function of z for the N and W nozzles, respectively. As a first-degree approximation, we applied a second-degree polynomial fit for τ (dashed curves) leading to R^2 values of 0.98 and 0.88 for the N and W nozzles, respectively. The variation of τ with z shows that the variation of d and v are not proportional, and while the decrease in d may be more pronounced than that of v for the shorter z (< 30 mm)—seen as a decrease in τ, the opposite is true for longer z (> 60 mm). We then use τ as a characteristic time to compute the non-dimensional residence time, t_r/τ, and non-dimensional spurt duration, $\Delta t/\tau$ for all our data. This results in a series of parallel curves when presented in a logarithmic plot, as shown in Figure 8 for the N nozzle.

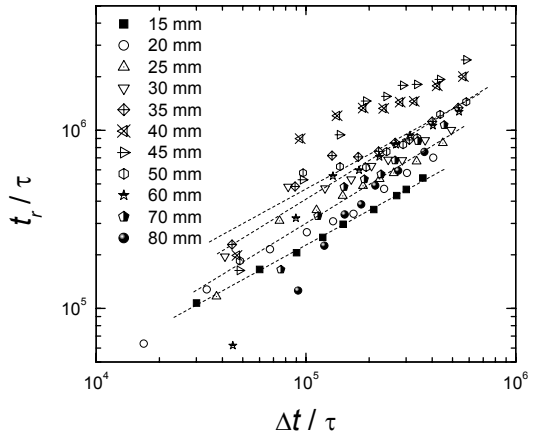

Figure 8. Dimensionless residence time versus dimensionless spurt duration for various z from 15 mm to 80 mm for the N nozzle. Dashed lines represent curve fits for some of the data shown in the graph.

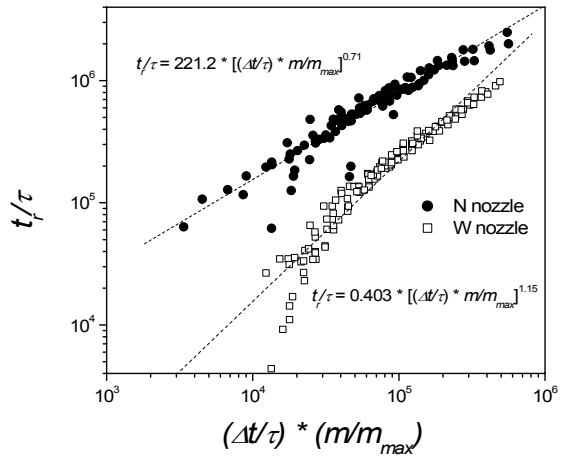

Figure 9. Dimensionless residence time plots for the N nozzle (solid symbols) and W nozzle (hollow symbols). For N nozzles only d and v data between z = 15-80 mm was used. For W nozzle, d and v data between z = 15 - 120 mm were used. Dashed curves are power laws fitting with R^2 = 0.9493 and 0.9622, for the N and W nozzles, respectively.

The strong dependence of these curves on z and their similar slope suggest the use of a free parameter, m/m_{max}, which is chosen in a way that all curves shown in Figures 5a and 5b are shifted with respect to that at z_{max}, thus collapsing into a single curve, as shown in Fig. 9 for both nozzles.

It is reasonable to think of this free parameter as an effective mass deposition ($m/m_{\max}$) which, due to the in-flight evaporation of spray droplets and the interaction of droplets with the surface, is also a function of z. Physically, m represents the local mass deposition, while m_{max} represents the maximal mass deposition at the distance $z_{max,}$ where t_r is maximal (z_{max} are 45 mm and 160 mm for the N and W nozzles, respectively.) As seen in Fig. 9, all the dimensionless residence time data can be very well approximated by two power laws, which are shown on Fig. 9 itself.

We may then take a step further and plot m/m_{max} *vs.* z to show the expected variation of m with z for each nozzle. Figure 10 shows the variation of m/m_{max} with z for both nozzles. Note that N nozzle shows a maximal m/m_{max} at z = 40 mm, while the W nozzle does not show until z ~ 150 mm. This is somewhat consistent with heat flux measurements (q) we have reported recently [26] for the N nozzle, which shows a maximum q at about z ~ 25-30 mm, suggesting that the effective mass deposition seen herein can be well correlated with the maximum heat flux.

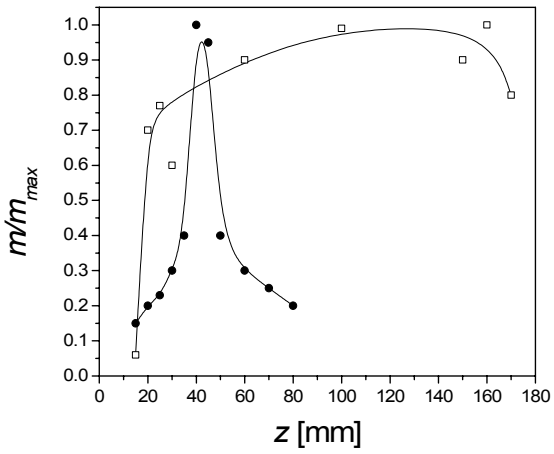

Figure 10. Dimensionless effective mass deposition as a function of z for the N (solid) and W nozzles (hollow). Notice that for the N nozzle, the mass deposition steadily increases reaching a maximum at z_{max} = 40 mm followed by a steady decrease, while the mass deposition for the W nozzle remains relatively constant after z >20 mm and only starts to decrease after z ~ 150 mm.

Table 2. Determination of τ from d and v. Values in shaded area were not used.

NARROW NOZZLE

z (mm)	d (μm)	v (m/s)	τ (x 10^7s)	z (mm)	d (μm)	v (m/s)	τ (x 10^7s)	z (mm)	d (μm)	v (m/s)	τ (x 10^7s)
15	13.27	40	0.33	55	10.60	43	0.25	85	10.53	32	0.33
30	13.60	62	0.22	60	10.32	44	0.23	90	11.14	30	0.37
35	10.11	46	0.22	65	10.35	41	0.25	105	15.46	27	0.57
40	9.76	45	0.22	70	10.32	37	0.28	120	17.71	21	0.84
45	9.00	45	0.20	75	10.42	33	0.32				
50	9.81	46	0.21	80	10.55	34	0.31				

WIDE NOZZLE

z (mm)	d (μm)	v (m/s)	τ (x 10^7s)	z (mm)	d (μm)	v (m/s)	τ (x 10^7s)	z (mm)	d (μm)	v (m/s)	τ (x 10^7s)
15	18.75	78	0.24	45	15.26	55	0.28	75	14.36	47	0.31
20	17.93	78	0.23	50	15.16	52	0.29	80	15.96	30	0.53
25	16.44	60	0.27	55	14.96	48	0.31	85	16.54	30	0.55
30	15.47	63	0.25	60	14.55	46	0.32	90	16.56	30	0.55
35	16.6	77	0.22	65	15.78	46	0.34	105	19.22	34	0.57
40	13.79	55	0.25	70	14.41	46	0.31	120	20.45	30	0.68

These studies have shown that there are large differences in the surface dynamics that occur between nozzles producing distinctive spray characteristics, which are clearly shown by the differences in t_r, T_{min}, z_c, and z_{max} for each nozzle. It is quite interesting that a surface parameter such as t_r can be easily correlated to Δt through the use of an appropriate spray characteristic time (τ) and an effective mass deposition factor (m/m_{max}). The present results represent a step towards a more complete understanding and quantification of the physics involved in CSC.

CONCLUSIONS

A fast response temperature sensor was used to determine the residence time (t_r) resulting from spurts with different spray characteristics. t_r gradually increases as a function of spurt duration (Δt) for increasing distance from the nozzle (z). However, at a critical distance (z_c), an abrupt increase occurs, suggesting a change in the spray pattern and/or spray-surface interactions. As z continues to increase, another critical distance (z_{max}) is reached, which can be associated with the distance of maximal cryogen deposition. Beyond that distance, the trend reverses and t_r decreases with increasing z. For the narrow (N) nozzle (0.7 mm inner diamter), z_c occurs at 35 - 40 mm and z_{max} occurs at 40 – 45 mm, while for the wide (W) nozzle (1.4 mm inner diamter), z_c is located at 15 – 20 mm and z_{max} at about 160 mm.

From the fundamental spray characteristics (d and v), a spray characteristic time was introduced, $\tau = d/v$ which is a

function of z. Using this parameter, the dimensionless residence time (t_r/τ) was plotted as a function of the product of the dimensionless spurt duration ($\Delta t/\tau$) and a dimensionless factor that we refer to as an effective mass deposition factor (m/m_{max}). In this fashion, all data collapsed into one for each nozzle and it could be very well approximated by simple power laws. The practical importance of these results is that it is shown that the effective mass deposition varies at different distances from the nozzle, which depends on the spray characteristics and, thus, on the nozzle geometry.

ACKNOWLEDGMENTS

This work was supported by the National Institutes of Health (GM62177 to JSN and HD42057 to GA). Institutional support from the Beckman Laser Institute Endowment is also acknowledged. Laboratory assistance provided by Emil Karapetian and Wole Olowu is greatly appreciated.

REFERENCES

[1] B. Anvari, T. E. Milner, B. S. Tanenbaum, S. Kimel, L. O. Svaasand, and J. S. Nelson, "Selective cooling of biological tissues: application for thermally mediated therapeutic procedures," *Phys Med Biol*, vol. 40, pp. 241-52, 1995.

[2] J. S. Nelson, T. E. Milner, B. Anvari, B. S. Tanenbaum, S. Kimel, L. O. Svaasand, and S. L. Jacques, "Dynamic epidermal cooling during pulsed laser treatment of port-wine stain. A new methodology with preliminary clinical evaluation," *Arch Dermatol*, vol. 131, pp. 695-700, 1995.

[3] C. J. Chang and J. S. Nelson, "Cryogen spray cooling and higher fluence pulsed dye laser treatment improve port-wine stain clearance while minimizing epidermal damage," *Dermatol Surg*, vol. 25, pp. 767-72, 1999.

[4] M.M. Elkobt, Fuel Atomization for Spray Modeling, Prog. Energy Combustion Sci., vol. 8, pp.16-91,1982.

[5] G.L. Hubbard, V.E. Denny and A.F. Mills, Int. J. Heat and Mass Transf., vol 16, pp.1003-1008,1973.

[6] W.E. Ranz and W.R. Marshall, Chem Eng. Prog., vol. 48, Part I, pp.141-146, Part II, pp.173-180, 1952.

[7] R.D. Ingebo, J. of Propulsion, July-August, vol. 7, pp.467-472, 1991.

[8] R.D. Ingebo RD, NASA Technical Memorandum 106106, prepared for the 29th Joint Propulsion Conference and Exhibit by the AIAA,SAE,ASME, and ASEE, Monterey, CA, June 28-30, 1993.

[9] R.D. Ingebo, NASA Technical Memorandum 105909, prepared for the 31st Aerospace Sciences Meeting and Exhibit by the AIAA,SAE, Reno, NV, January 11-14, 1993.

[10] G. Aguilar, G. X. Wang, and J. S. Nelson, "Dynamic behavior of cryogen spray cooling: Effects of spurt duration and spray distance," La*sers in Surgery and Medicine,* vol. 32, pp. 152-159, 2003.

[11] J. H. Torres, J. S. Nelson, B. S. Tanenbaum, T. E. Milner, D. M. Goodman, and B. Anvari, "Estimation of internal skin temperatures in response to cryogen spray cooling: Implications for laser therapy of port wine stains," Ie*ee Journal of Selected Topics in Quantum Electronics,* vol. 5, pp. 1058-1066, 1999.

[12] J. W. Tunnell, J. H. Torres, and B. Anvari, "Methodology for estimation of time-dependent surface heat flux due to cryogen spray cooling," An*n Biomed Eng,* vol. 30, pp. 19-33, 2002.

[13] B. Majaron, G. Aguilar, B. Basinger, L. L. Randeberg, L. O. Svaasand, E. J. Lavernia, and J. S. Nelson, "Sequential cryogen spraying for heat flux control at the skin surface," presented at SPIE, San Jose CA, 2001.

[14] G. Aguilar, B. Majaron, K. Pope, L. O. Svaasand, E. J. Lavernia, and J. S. Nelson, "Influence of nozzle-to-skin distance in cryogen spray cooling for dermatologic laser surgery," La*sers in Surgery and Medicine,* vol. 28, pp. 113-120, 2001.

[15] B. Anvari, B. S. Tanenbaum, T. E. Milner, S. Kimel, L. O. Svaasand, and J. S. Nelson, "A theoretical study of the thermal response of skin to cryogen spray cooling and pulsed laser irradiation: implications for treatment of port wine stain birthmarks," Ph*ys Med Biol,* vol. 40, pp. 1451-65, 1995.

[16] B. Majaron, L. O. Svaasand, G. Aguilar, and J. S. Nelson, "Intermittent cryogen spray cooling for optimal heat extraction during dermatologic laser treatment," Ph*ysics in Medicine and Biology,* vol. 47, pp. 3275-3288, 2002.

[17] G. Aguilar, W. Verkruysse, B. Majaron, L. O. Svaasand, E. J. Lavernia, and J. S. Nelson, "Measurement of heat flux and heat transfer coefficient during continuous cryogen spray cooling for laser dermatologic surgery," Ie*ee Journal of Selected Topics in Quantum Electronics,* vol. 7, pp. 1013-1021, 2001.

[18] G. Aguilar, B. Majaron, W. Verkruysse, Y. Zhou, J. S. Nelson, and E. J. Lavernia, "Theoretical and experimental analysis of droplet diameter, temperature, and evaporation rate evolution in cryogenic sprays," In*ternational Journal of Heat and Mass Transfer,* vol. 44, pp. 3201-3211, 2001.

[19] B. M. Pikkula, J. H. Torres, J. W. Tunnell, and B. Anvari, "Cryogen spray cooling: Effects of droplet size and spray density on heat removal," La*sers Surg Med,* vol. 28, pp. 103-12, 2001.

[20] E. Karapetian, G. Aguilar, S. Kimel, E. J. Lavernia, and J. S. Nelson, "Effects of mass flow rate and droplet velocity on surface heat flux during cryogen spray cooling," Ph*ysics in Medicine and Biology,* vol. 48, pp. N1-N6, 2003.

[21] G. Aguilar, G. X. Wang, and J. S. Nelson, "Effect of Spurt Duration on the Heat Transfer Dynamics during Cryogen Spray Cooling," Ph*ysics in Medicine and Biology,* vol. 48, pp. 2169-2181, 2003.

[22] Bachalo, W. D. Applied Optics 1980, 19, 360-370.

[23] A.H. Lefebvre, "Atomization and Sprays", 1st ed., New York NY, Taylor & Francis, 1989.

[24] M. Orme, "Experiments on droplet collisions, bounce, coalescence and disruption", Progress in Energy and Combustion Science, vol. 23, pp. 65-79, 1997.

[25] R. Nishitani, A. Kasuya, and Y. Nishina, "Insitu STM observation of coalescence of metal particles in liquid", Zeitschrift fur Physik D- Atoms, Molecules and Clusters, vol. 26, pp. S42-S44, 1993.

[26] G.X. Wang, G. Aguilar, and J. S. Nelson, "Effect of Nozzle Distance on the Dynamic Surface Heat Transfer during Cryogen Spray Cooling", submitted to Int. J. of Heat and Mass Transfer, May 2003.